Influence of Measured Freestream Disturbances on Hypersonic Boundary-Layer Transition

R. D. WAGNER JR.,* D. V. MADDALON,† AND L. M. WEINSTEIN‡
NASA Langley Research Center, Langley Station, Hampton, Va.

Results of a study of transition in hypersonic flow over a wide range of test conditions in the Langley $M = 20$ helium tunnel are presented. Direct measurements of the facility freestream disturbances have been made with a constant current anemometer. In unheated flow, the interpretation of fluctuation mode diagrams identify the disturbances as sound waves produced by moving sources of sound (the turbulent nozzle wall boundary layer). The test section disturbance levels can be quite high with a maximum of about 3.5% rms mass flow fluctuation (which corresponds to about 6% rms static pressure fluctuation) when transition of the nozzle wall boundary layer occurs in the portion of the nozzle that can influence the test section disturbance level via direct acoustic radiation. For the same range of test conditions, transition measurements have been made on a 10° half-angle wedge. A strong correlation between the movement of transition on the model and the freestream disturbance level is observed; transition appears to be dominated by the intense sound radiation of the nozzle wall boundary layer. The results show that the freestream disturbances are a major contributor to the commonly referred to unit Reynolds number effect on transition Reynolds number.

Nomenclature

A_w = overheat parameter
C = wire thermal capacity, joules/°R
d = wire diameter, ft
E' = finite circuit parameter
$E(f)$ = normalized power spectra (Hz)$^{-1}$
e = voltage fluctuation across hot wire, mv
Δe_m = sensitivity to mass flow
Δe_t = sensitivity to stagnation temperature
f = frequency, Hz
h = film coefficient of heat transfer, Btu/ft^2-sec-°R
I = hot-wire heating current, ma
i.d. = tube inside diameter, in.
K = $d \log R_w / d \log T_w$
k = heat conductivity, Btu/ft-sec-°R
M = Mach number
$\mathfrak{M}$ = time constant, sec
m = ρv, lbm/ft^2-sec
NU_0 = hd/k_{t_∞} = Nusselt number
o.d. = tube outside diameter, in.
P = pressure, psig or psia
$\dot{q}$ = heating rate, Btu/ft^2-sec
R = Reynolds number
R/in. = unit Reynolds number
R_{e_0} = $\rho_\infty v_\infty d/\mu_{t_\infty}$
R_{mt} = correlation of mass flow and total temperature fluctuations
R_r = reference resistance, ohm
R_w = wire resistance, ohm
r = sensitivity ratio
T = temperature, °R
T_r = reference temperature, °R
V = mean hot-wire voltage, mv
v = velocity, fps
X = overheat parameter
x = distance from model nose or tunnel throat along surface, in.
Y = fluctuation parameter
y = perpendicular distance from wall, in.
α = $\{1 + [(\gamma - 1)/2]M_\infty^2\}^{-1}$
α_r = temperature resistivity coefficient
β = $(\gamma - 1)M_\infty^2\alpha$
γ = specific heat ratio
δ = boundary-layer thickness, in.
δ^* = displacement thickness, in.
ϵ = finite circuit factor
η = wire recovery factor (T_w/T_{t_∞} at $I = 0$)
θ = momentum thickness, in.
μ = viscosity, lbm/ft-sec
π = pressure mode amplitude
ρ = density
σ = entropy mode amplitude
τ_{wr} = temperature loading, $(T_w - \eta T_t)/\eta T_t$

Subscripts

2 = behind normal shock wave
e = boundary-layer edge
FP = flat-plate value
s = source
SP = surface Pitot tube
T = beginning of transition from heating rate
T' = beginning of turbulent flow (peak heating)
TC = corrected for transverse curvature
TS = test section conditions, station 139
t = total
w = wall or hot wire
x = distance, in.
∞ = freestream, ahead of shock wave

Superscripts

$(\tilde{\ })$ = root mean square
$(\bar{\ })$ = time average value
$(\ )'$ = instantaneous value

Presented as Paper 69-704 at the AIAA Fluid and Plasma Dynamics Conference, San Francisco, Calif., June 16–18, 1969; submitted June 19, 1969; revision received February 20, 1970.

* Aerospace Engineer; presently Program Manager, Research Section, NASA Headquarters, Washington, D.C. Member AIAA.
† Aerospace Engineer, Aero-Physics Section. Associate Member AIAA.
‡ Aerospace Engineer, Aero-Physics Section.

I. Introduction

IN supersonic flow, Kovasznay[1] shows that three disturbance modes can theoretically exist: 1) temperature spottiness, 2) vorticity, and 3) sound radiation. In supersonic (or hypersonic) tunnels, temperature spottiness and vorticity (the latter is usually dominant in low-speed flows) are introduced in the supply and stagnation chamber and convected along streamlines into the nozzle and the test section. Diffusion across streamlines of these two modes should be relatively unimportant, and for $M > 2$, the vorticity introduced in the supply or stagnation chamber is diminished to a negligible amount in the test section because of the nozzle expansion (see Refs. 2 and 3). With no heating of the supply gas, the flow should be near adiabatic with negligible temperature spottiness; for a heated gas supply, this may not be the case.

When turbulent boundary layers exist on the nozzle walls, a sound field with a preferred orientation (not the freestream Mach wave orientation) radiates into the nozzle. Though this phenomenon has been studied by Laufer,[4] not enough is known to predict with confidence the intensity of this sound or its gross characteristics. It thus seems that one can only speculate that both sound and temperature spottiness may occur in hypersonic nozzles and the extent of each may be peculiar to the facility in which transition measurements are made.

Evidence exists that the primary cause for much of the confusion in the study of high Mach number transition has been the insufficient knowledge of all factors affecting transition. The freestream disturbance levels of the test facilities are suspected to be of prime importance and may be a major contributor in the enigmatic unit Reynolds number effect on transition Reynolds number. Experimental results supporting this proposition were presented by Pate and Schueler[5] (wherein stream disturbance levels are inferred from model wall static pressure fluctuation measurements). Still, direct measurements of the stream disturbances together with transition measurements are needed to confirm the importance of the stream disturbance levels, and to assure that disturbance modes other than sound have not been overlooked.

The present objective was to provide a confirming experiment that sound radiation from the turbulent nozzle wall boundary layer plays a dominant role in hypersonic model boundary-layer transition. To accomplish this objective, transition was studied in hypersonic flow over the range of available test conditions of the Langley $M = 20$ helium tunnel with a detailed knowledge of the stream disturbances obtained by direct measurement with a constant current anemometer.

II. Facility, Transition Model, and Hot-Wire Instrumentation

Test Facility

The experiments were conducted in the Langley $M = 20$ hypersonic helium tunnel. This tunnel has a contoured nozzle and a 22-in.-diam test section. The freestream Mach number in the test core, though constant at any given stagnation pressure (i.e., the axial and lateral Mach number gradients are negligible in the test core), varies with stagnation pressure from a low of 16.2 at 75 psia to 21.7 at 3015 psia. A calibration and description of the facility is given in Ref. 6.

Transition Model

The model was a sharp leading edge (approximately uniform 0.002 in. thick), smooth, 10° half-angle wedge with an 11-in. span and a 24-in. chord. It was fabricated of Inconel 600 with a wall thickness of 0.030 in. and had swept end plates. Forty-three thermocouples placed along the model center line and spaced about 0.5 in. apart were used to determine heating rates and, thence, transition location. The model wall temperature was initially uniform at 540°R and changed only slightly during a test.

Hot-Wire Instrumentation

The hot-wire system was a commercially available constant current anemometer with frequency response up to 500 kHz. The hot-wire probes (see Figs. 1a and b) consisted of two needles embedded in a wedge-shaped holder. The holder was cast from a high-temperature epoxy with the needle tips

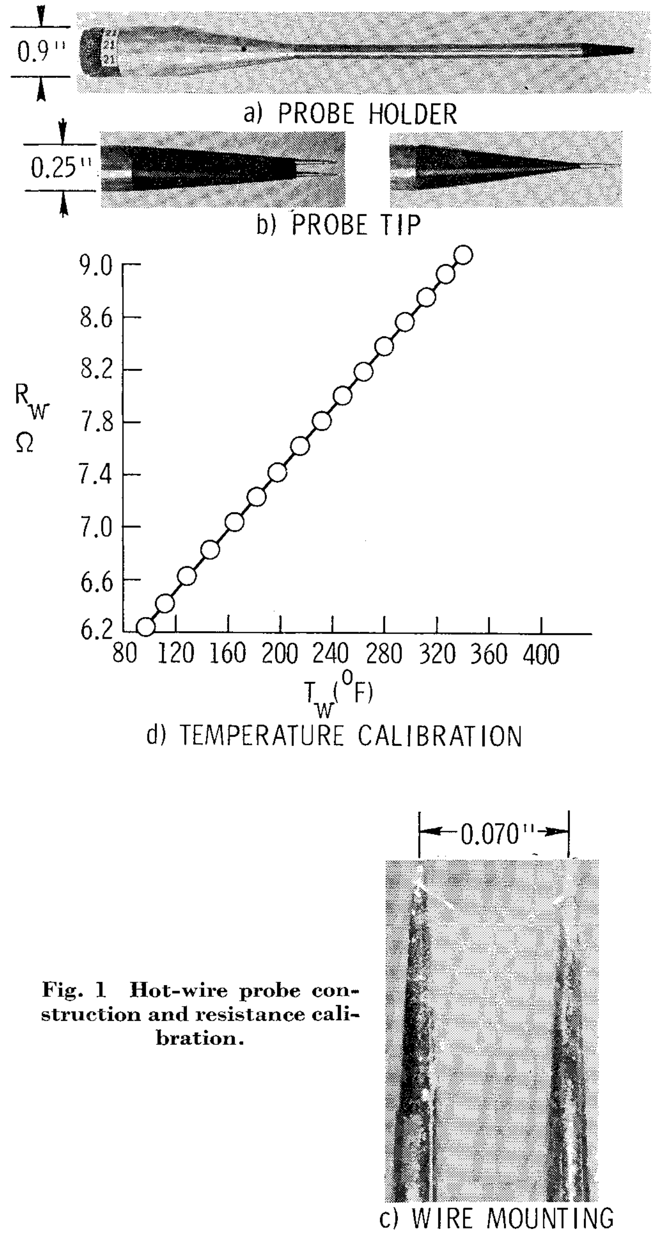

Fig. 1 Hot-wire probe construction and resistance calibration.

spaced about 0.070 in. apart. One and one-half tenths mil (0.00015 in.) tungsten wire was used for the hot wire. The ends of the tungsten wires are first electroplated with copper; the plating was then tinned and soft-soldered to the needles. The remaining unplated portion of the wire is centered at midspan and is about 0.045 in. long (the sensitive part of the wire thus having an aspect ratio of about 300). Some detail can be seen in the photograph taken through a microscope in Fig. 1c. The problem of strain-gage oscillations was the most troublesome experienced in making hot-wire probes. Typically, 15 of 16 visually acceptable probes had to be rejected because of strain-gage oscillations. About a quarter-circle slack was used to help avoid strain-gage oscillations; the nonsensitive copper-plated portion of the wires (extending beyond the needle shock waves) was also believed to be essential. This portion of wire (the larger diameter plated wire) intersected the needle shock wave which produced signals similar to strain-gage oscillations on unplated wires. Probes without these extensions always had intense oscillations.

For acceptance checking and calibration of hot-wire probes, a 3-in. exit diameter conical nozzle, using the 22-in. tunnel high-pressure helium supply and vacuum system, was invaluable. This 3-in. tunnel could be operated over near the

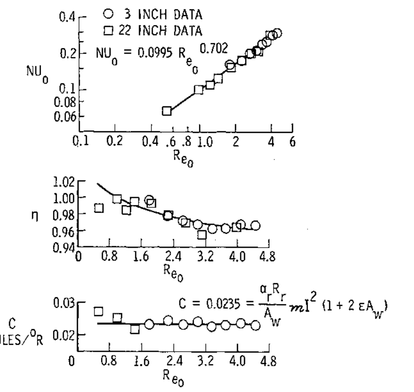

Fig. 2 Typical hot-wire calibration.

same range of test conditions as the 22-in. tunnel, but with essentially continuous running time. The hot-wire probes were first checked for strain-gage oscillations in the 3-in. tunnel and, if a panoramic wave analyzer showed a clean signal, the wire was then subjected for several minutes to the maximum stagnation pressure and heating current to be experienced in the test.

The wires were then placed in a temperature calibration oven containing a nonoxidizing atmosphere, pressurized helium, and calibrated for resistance vs temperature. A typical calibration is shown in Fig. 1d. Over the range of wire temperature obtained in these tests, a linear variation of resistance with temperature was quite satisfactory (<1% error), or

$$R_w = R_r[1 + \alpha_r(T_w - T_r)] \qquad (1)$$

After oven calibration, the wires were then flow calibrated in the 3-in. tunnel for heating rate and recovery factor variation with flow conditions. These calibrations, supplemented by calibration data generated in the tests in the 22-in. tunnel, were used to calculate the sensitivities of the hot wire (for the disturbance measurements) as shown by Morkovin in Ref. 7. Calibration differences for wires having the same resistance at room temperature were small. Still, each wire was individually calibrated rather than the usual method of using a universal infinite wire calibration and making end loss corrections (see, i.e., Dewey[8] and Vrebalovich[9]) because, first, a universal curve for supersonic helium flow is not available in the literature and, second, the wire slack would make uncertain any end loss corrections. The individual calibration method was used by Demetriades[10] with good results.

For hypersonic flow the Nusselt number based on stagnation temperature, $NU_0 = hd/k_{t_\infty}$, and the recovery factor, $\eta = T_r/T_{t_\infty}$, are independent of Mach number and depend only on the Reynolds number based on stagnation viscosity,[8] $R_{e_0} = (\rho_\infty v_\infty d)/\mu_{t_\infty}$. A typical calibration for NU_0 and η in terms of R_{e_0} is given in Fig. 2. In the figure are data from the 3-in. tunnel and also that data generated during fluctuation measurements in the 22-in. tunnel. Over the operating range, the NU_0 can be fitted with a power law in R_{e_0}.

Because of the short running time (about 50 sec) and approximately 3-hr pump-up cycle of the 22-in. tunnel, measurement of the hot-wire time constant $\mathfrak{M}$ at each of the heating currents in a run is not practical. To avoid the time consuming and costly measurement at even one heating current (usually four 50-sec runs were required to get an accurate measurement of $\mathfrak{M}$ in the 22-in. tunnel), the wire time constant was calibrated in the 3-in. tunnel where running time presented no problem. Time constants were measured over a range of flow conditions in the 3-in. tunnel, and the theoretical expression developed by Morkovin[7] was used to predict the wire thermal capacity C;

$$C = (\alpha_r R_r/A_w)\mathfrak{M}I^2(1 + 2\epsilon A_w) \qquad (2)$$

where A_w is Morkovin's overheat parameter, $A_w = \frac{1}{2}\partial \log R_w/\partial \log I$, I is the wire current, $\mathfrak{M}$ is the time constant, and ϵ is the finite circuit factor. In Fig. 2 a typical calibration for C is shown; measurements at the low values of R_{e_0} in the 22-in. tunnel are also given. The near constancy of the predicted thermal capacity of the wire and the discussion in Morkovin and Phinney[11] give credence to this method of predicting the wire time constant. For 22-in. tunnel experiments, the predicted wire time constant [from Eq. (2)] at zero heating current was set in the compensating amplifier at all currents. The rms data were then corrected using the formula

$$\tilde{e}_{\text{true}}/\tilde{e}_{\text{amp}} = \mathfrak{M}_{\text{true}}/\mathfrak{M}_{\text{amp}} \qquad (3)$$

where $\tilde{e}_{\text{true}}$ is the rms voltage at the correct time constant $\mathfrak{M}_{\text{true}}$ and $\tilde{e}_{\text{amp}}$ is the rms voltage measured in the tests with the zero heating current time constant $\mathfrak{M}_{\text{amp}}$ set in the compensating amplifier. This leads to some signal distortion at low frequencies on the order of the wire rolloff frequency (always <1000 Hz), but this effect should be negligible.

With the thermal inertia of the wire accounted for in both the time constant measurements and the signal correction, as noted, the basic hot-wire equation showing the fundamental sensitivity of the hot wire to mass flow and total temperature fluctuations is

$$e'/V = \Delta e_t T_t'/\bar{T}_t - \Delta e_m m'/\bar{m} \qquad (4)$$

where e', T_t', and m' are the instantaneous fluctuations in wire voltage, total temperature, and mass flow; V, $\bar{T}_t$, and $\bar{m}$ are the time average values. The wire sensitivities are given by Morkovin[7]

$$\Delta e_m = E'[A_w \partial \log NU_0/\partial \log R_{e_0} - (A_w/\tau_{wr})\partial \log\eta/\partial \log R_{e_0}] \qquad (5)$$

and

$$\Delta e_t = E'[K + A_w\{K - 1.647 + 0.647\partial \log NU_0/\partial \log R_{e_0} - (0.647/\tau_{wr})\partial \log\eta/\partial \log R_{e_0}\}] \qquad (6)$$

where the high Mach number independence and helium gas constants have been inserted. E' is the finite circuit parameter, and τ_{wr} is the temperature loading, $(T_w - T_r)/T_r$.

Modal analysis of the rms mass flow and total temperature fluctuations can be made as suggested by Kovasznay[12] by observing a virtual total temperature fluctuation, $\tilde{e}/V\Delta e_t$, at several sensitivites, $r = \Delta e_m/\Delta e_t$. From Eq. (4),

$$(\tilde{e}/V\Delta e_t)^2 = (\tilde{T}_t/\bar{T}_t)^2 - 2r(\tilde{T}_t/\bar{T}_t)(\tilde{m}/\bar{m})R_{mt} + r^2(\tilde{m}/\bar{m})^2 \qquad (7)$$

where R_{mt} is equal to the time average of the product, $m'T_t'$, divided by the product, $\tilde{m}\tilde{T}_t$. In each test, the hot wire was

Table 1 Summary of tunnel wall boundary-layer surveys at station 139 with $T_w/T_{t\infty} \approx 1.0$ (pressure probe o.d. = 0.125, i.d. = 0.100 in.)[a]

M_∞	Pt_∞, psia	R_∞/in. $\times 10^6$	T_{t_∞}	δ^*_{FP}	δ_{TC}	θ_{FP}	θ_{TC}	δ
16.2	75	0.051	510	5.38	5.26	0.0250	0.0176	7.5
16.9	120	0.079	520	5.88	5.73	0.0251	0.0169	8.2
17.1	165	0.108	530	5.29	5.10	0.0226	0.0158	7.9
17.5	225	0.146	545	5.18	4.95	0.0217	0.0153	7.9
17.9	275	0.171	546	4.96	4.81	0.0200	0.0144	8.0
18.2	315	0.194	546	4.82	4.61	0.0190	0.0137	8.0
18.6	365	0.220	549	4.69	4.49	0.0177	0.0130	7.5
18.7	415	0.248	550	4.57	4.42	0.0174	0.0130	7.5
18.8	465	0.278	550	4.54	4.30	0.0172	0.0127	7.5
19.1	515	0.302	552	4.28	4.09	0.0157	0.0118	7.8
19.5	615	0.350	555	3.99	3.83	0.0144	0.0111	7.9
19.8	765	0.423	562	3.90	3.73	0.0137	0.0107	7.7
20.3	1015	0.548	563	3.70	3.53	0.0125	0.0098	7.2
21.6	2015	1.010	566	2.94	2.84	0.0090	0.0075	5.4
22.2	3015	1.412	582	2.72	2.64	0.0079	0.0067	5.2

[a] Note: R_∞/in. based on viscosity corrected for low-temperature quantum effects.

operated through 7 to 10 currents, that is, 7 to 10 values of r. This yields redundant information to determine the three unknowns, $\tilde{T}_t$, $\tilde{m}$, and R_{mt}, for that particular test. The repeatability of measurements with a single wire was about $\pm 5\%$.

III. Definition of Tunnel Flow

Boundary-Layer Surveys

The evidence to date indicates that acoustic radiation from turbulent tunnel wall boundary layers may be the major contributor to freestream disturbances in supersonic and hypersonic tunnels. For this reason, consideration was given to the nature of the tunnel wall boundary layer. Pitot tube surveys of the tunnel wall boundary layer were made in the test section (station 139) with unheated flow for the test conditions summarized in Table 1. Though the flow was unheated, some variation of stagnation temperature with stagnation pressure occurs because of the inverse Joule-Thompson effect observed in throttling high pressure helium. This effect is most pronounced at high stagnation pressures for which the highest supply pressure was used. This real gas effect should not give rise to temperature spottiness in the flow.

The results of three representative surveys are shown in Fig. 3 with y, the distance from the wall, referenced to the displacement thickness. The velocity profiles were calculated from the Pitot pressure data, assuming constant static pressure and total temperature through the boundary layer. Displacement thickness and momentum thickness calculated with (subscript, TC) and without (subscript, FP) a transverse curvature correction[13] are summarized in Table 1. The transverse curvature correction (a correction for the thin boundary-layer assumption in the flat plate solution) has little effect on δ^* but reduces θ by as much as 35%. The tunnel wall boundary-layer edge δ, defined as the point where Pitot pressure reached a constant value, is also given in Table 1.

A flat plate similar solution (computed by the method of Cohen[14]) is shown with the velocity profiles in Fig. 3; a $\frac{1}{9}$-power law representative of turbulent flow is also given. The velocity profile at 75 psia appears transitional compared to the laminar theory and the higher pressure profiles; the high-pressure profiles are fuller than the $\frac{1}{9}$-turbulent-type profile. These data indicate that over the tunnel operating range, transition occurs in the nozzle wall boundary layer with the transition point moving up the nozzle as the stagnation pressure increases. This suggests that at sufficiently low stagnation pressures, that portion of the nozzle wall boundary layer that could influence the disturbance level in the central region of the test section via direct acoustic radiation (i.e., within the Mach cone) may be laminar with a much reduced disturbance level in the test section as a result. To examine this possibility, surface Pitot pressures were measured on the tunnel wall.

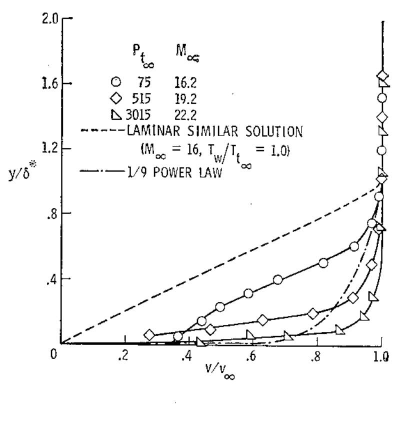

Fig. 3 Tunnel wall boundary-layer velocity profiles at station 139.

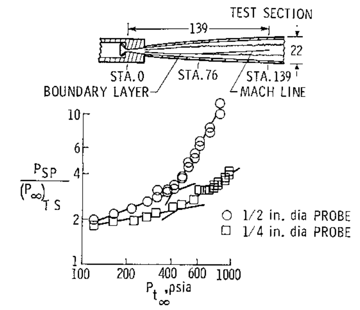

Fig. 4 Surface Pitot pressure on nozzle wall (station 76).

Surface Pitot Surveys

Measurements of surface Pitot pressure were taken at a station 76 in. downstream of the throat; the test core Mach number at this station is nearly equal to that at station 139. Station 76 is the approximate location in the nozzle where disturbances in the outer region of the boundary layer could produce direct acoustic radiation into the central part of the test section (see top of Fig. 4). This part of the nozzle will be referred to as the "acoustic origin." Boundary-layer surveys at this station were not made, due to access problems. The surface Pitot pressure measurements for two different size probes are in Fig. 4. Both probes clearly indicate a change in the nature of the tunnel wall boundary layer at a stagnation pressure of about 400 psia. Near this stagnation pressure, the pitot pressure began to fluctuate. In Fig. 4, two symbols at a given pressure indicate the range of these fluctuations. These two effects are interpreted as indications of transition from laminar to turbulent flow in the tunnel wall boundary layer at station 76.

Freestream Disturbance Measurements

To study the disturbances in the test section, the hot wire was placed near the tunnel center line at a station 139 in. from the throat. Hot-wire surveys across the test section at a fixed current showed a near constant $\tilde{e}$ outside of the tunnel wall boundary layer as also observed at low Mach numbers.[4] Kovasznay-type mode diagrams were made over the range of operating pressures. All of these diagrams were made with one unusual wire which survived 17 runs. Some representative diagrams are shown in Fig. 5. All the mode diagrams were linear with a positive slope which means that the correlation of m' and T_t', R_{mt} was -1; that is, the mass flow and total temperature fluctuations are correlated. This follows from Eq. (7) which is factorable for this condition,

$$\tilde{e}/V\Delta e_t = \tilde{T}_t/\bar{T}_t + r(\tilde{m}/\bar{m}) \tag{8}$$

The slope of the mode diagram is the rms of the fluctuation of mass flow divided by the mean, and the intercept at $r = 0$ is the rms of the fluctuation in total temperature divided by the mean. In Fig. 6 the rms of the fluctuations in mass flow and total temperature are shown for unheated flow over the range

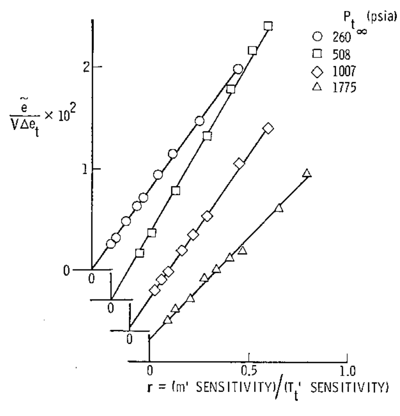

Fig. 5 Fluctuation mode diagrams of freestream disturbances at station 139.

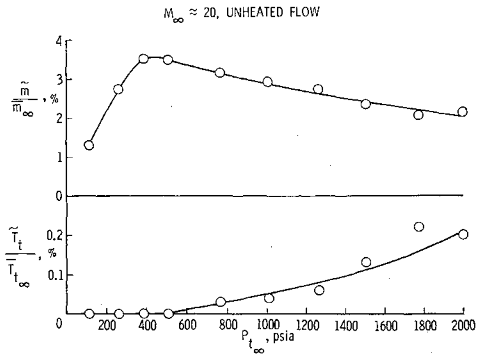

Fig. 6 Freestream rms mass flow and total temperature levels at station 139.

of operating pressures. At about 400 psia, where the surface Pitot pressures indicated the initiation of transition at station 76, the rms of the fluctuation of mass flow reaches a maximum of about 3.5%. The value of $\tilde{m}/\bar{m}_\infty$ falls off rapidly below 400 psia to just over 1% at the lowest pressure (115 psia) for which a mode diagram was made. At 65 psia, no signal above the instrument noise could be distinguished. Laufer[4] found that mass flow fluctuations decreased by a factor of 10 when the tunnel wall boundary layer changed from turbulent to laminar. Above 400 psia a more gradual fall-off occurs in the percent mass flow rms fluctuations. The magnitudes of these mass flow fluctuations are quite large, the maximum being about three times higher than the maximum measured by Laufer[4] at $M_\infty = 5$, who also found that $\tilde{m}/\bar{m}$ increases with Mach number. The total temperature fluctuations are at least an order of magnitude smaller than the mass flow fluctuations and appear to exist only after transition has moved through the acoustic origin, that is, at pressures above 400 psia. These total temperature fluctuations are believed to originate not in the stagnation chamber or supply (with unheated flow, one would not expect any temperature spottiness) but to be caused by the tunnel wall boundary-layer turbulence, as will become apparent subsequently.

Disturbance Spectra

Normalized hot-wire power spectra are shown in Fig. 7. These data were obtained by recording the hot-wire compensated signal on a wide-band, FM tape recorder (d.c. to 400 kHz) and replaying the record into a wave analyzer. For each stagnation pressure, a signal sample about 40 sec long was recorded with the wire heating current set to give $r \approx 0.35$. In all cases, the bulk of the signal (at least 90%) lies below 100 kHz; for this reason, the spectra of Fig. 7 are shown only up to 70 kHz. Clearly, the signals were not demanding of the instrumentation frequency response.

At the lower stagnation pressures, where surface Pitot pressures indicate the tunnel wall boundary layer is laminar at the acoustic origin, the power spectra show the energy to be concentrated in the low frequencies, below about 20 kHz. In fact, the signal spectrum at 115 psia was lost in the instrument noise beyond about 70 kHz. When the tunnel wall boundary layer becomes turbulent (the two highest pressures in Fig. 7), the power spectra have proportionately much more energy at high frequencies. At $P_{t_\infty} = 1015$ psia and above, the spectra showed some signal above the instrument noise out to 400 kHz; though, as previously stated, the major portion of the energy was still below 100 kHz.

Interpretation of Disturbance Measurements

The interpretation of the disturbances in terms of a simple disturbance mode follows the analysis made in Ref. 4. The observed correlation of m' and T_t', $R_{mt} = -1$, rules out the possibility that the disturbances measured could be caused by vorticity fluctuations for which $R_{mt} = +1$. For pure temperature spottiness $R_{mt} = -1$ but, in this case, all the straight-line mode plots should then have a preferred horizonal intercept of $r = -\alpha$ at $\tilde{e}/V\Delta e_t = 0$, where $\alpha = \{1 + [(\gamma - 1)/2]M_\infty^2\}^{-1}$. A representative value of α is about 0.01. The mode diagrams for high stagnation pressure (illustrated by the data at 1775 psia in Fig. 5) clearly did not have $-\alpha$ for an intercept. For the intermediate pressures (about 1000 psia) the mode diagrams could be faired through $r = -\alpha$; but at the low pressures (500 psia and below) the mode diagrams consistently favored an $r = 0$ horizontal intercept, though exclusion of the $r = -\alpha$ horizontal intercept is not distinct. Recalling that no signal was observed at 65 psia, this implies that temperature spottiness exists only at a given pressure level. With unheated flow, no mechanism is known which could produce such an effect, and such an interpretation would seem unreasonable. Furthermore, a cogent reason for rejecting temperature spottiness is that in the following paragraph an alternative interpretation is discussed which is consistent with other experimental observations.

The other alternative is a pure sound field with a preferred orientation which also produces linear mode diagrams with $R_{mt} = -1$. In this case, a finite total temperature fluctuation implies that the sound originates from a moving source, and the wave front orientation is not that of a freestream Mach wave.[4] A stationary source of sound, a fluctuating Mach wave, for example, would have zero total temperature fluctuation; that is, moving sources of sound produce total temperature fluctuations. With this interpretation, the percent rms pressure fluctuations and the source velocities for the sound waves are shown in Fig. 8. (The large degree of uncertainty for the source velocity at the lower pressures will be explained subsequently.) This interpretation of the data forms a consistent picture with the surface Pitot pressure measurements and the variations of the hot-wire signal spectra. When transition moves through the acoustic origin, a sound disturbance is established that is either stationary or moving at somewhat less than stream velocity. At higher pressures, when a turbulent type of spreading of the hot-wire

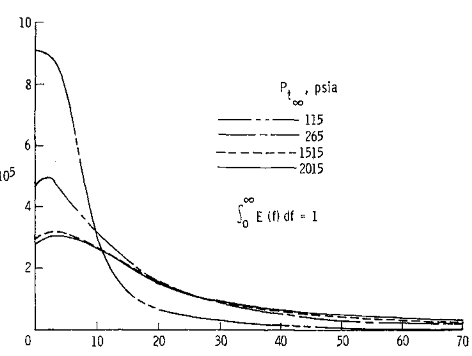

Fig. 7 Freestream normalized power spectra of hot-wire signal at station 139.

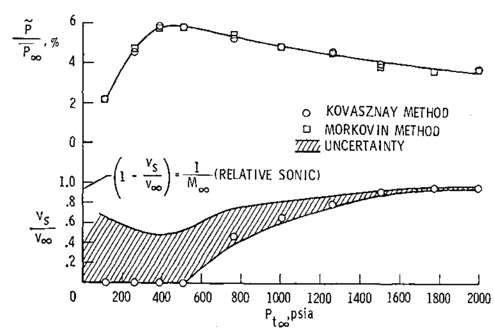

Fig. 8 Freestream rms pressure fluctuation and disturbance source velocity at station 139.

signal spectra is observed, a turbulent boundary layer exists in the nozzle and radiates as a moving source of sound. The source velocity approaches freestream velocity and the sound intensity decreases as stagnation pressure (or R_∞/in.) increases at the higher pressures. For fully turbulent flow at $M_\infty = 5$ (Ref. 15), the intensity was also observed to diminish with increasing R_∞/in., but the source velocities are only about 0.6 v_∞. The pressure fluctuations given in Fig. 8 are quite high, nearly 6% of freestream pressure in the transitional pressure range about 400 psia.

As a consistency check on the data, a somewhat different modal decomposition of the data was made using the parameters introduced by Morkovin.[7] These parameters relate the hot-wire signal directly to the fundamental mode variables δ, τ, and π, the entropy (temperature spottiness), vorticity, and pressure mode amplitudes, respectively. These parameters are $Y = e'/V\Delta e_\sigma$ and $X = \Delta e_\tau/\Delta e_\sigma$. Δe_σ and Δe_τ are the sensitivities to σ and τ, respectively,

$$\Delta e_\sigma = \Delta e_m + \alpha \Delta e_t \tag{9}$$

$$\Delta e_\tau = \beta \Delta e_t - \Delta e_m \tag{10}$$

Mode diagrams using these variables are shown in Fig. 9. The $X = 0$ intercepts (when interpreted as sound waves) give the value of $\tilde{\pi} = \tilde{P}/\gamma\bar{P}$ and the slope of the straight-line mode diagram is related to the source velocity, or equivalently, the sound wave orientation. The pressure fluctuations from these diagrams (which tend to emphasize the lower values of r whereas Kovasznay's variables emphasize the high values of r) agree with those determined by the Kovasznay diagrams (see Fig. 8). Source velocities were not determined from this method, however, because of the extremely small slopes involved; a fluctuating Mach wave (stationary source of sound) would give an intercept, $Y = 0$, at $X = (\gamma - 1)M_\infty^2$ or on the order $X = 200$ for these tests. A disturbance of pure temperature spottiness would give a constant Y for all X in these variables.

At very high Mach number, with the hot wire, it becomes difficult to distinguish between sound waves from a stationary source (or from sources moving at much less than freestream velocity) and temperature spottiness. The distinguishing feature between the two modes is the velocity fluctuations which are present in the sound waves. However, the hot wire is sensitive only to the velocity fluctuation component in the mean flow direction. Since the velocity fluctuations in a sound wave are normal to the wave front, for slow moving sources where the wave fronts are near parallel to the mean flow (in hypersonic flow), the hot wire becomes insensitive to the velocity fluctuation and hence the orientation (or source velocity) cannot be resolved. A result of this is the large uncertainty indicated in Fig. 8 at the lower velocities. Using the sound wave relations of Ref. 4, it is easily shown that the total temperature fluctuation, mass flow fluctuation, and source velocity are related as follows for hypersonic flow:

$$\tilde{T}_t/\bar{T}_t \sim [2(v_s/v_\infty)\tilde{m}/\bar{m}]/M_\infty^2(1 - v_s/v_\infty) \tag{11}$$

Equation (11) clearly shows that the source velocity determination from measurements of $\tilde{m}/\bar{m}$ and $\tilde{T}_t/\bar{T}_t$ (for a fixed resolution of $\tilde{m}/\bar{m}$ and, particularly, $\tilde{T}_t/\bar{T}_t$) is most accurate for source velocities near freestream velocity due to the singularity in $\tilde{T}_t/\bar{T}_t$ at $v_s/v_\infty = 1$. The small $\tilde{T}_t/\bar{T}_t$ induced by the slow moving sources (note $\tilde{T}_t/\bar{T}_t = 0$ for $v_s/v_\infty = 0$), which was comparable to the $\tilde{T}_t/\bar{T}_t$ resolution at low stagnation pressures, explains the greater uncertainty at lower pressure in Fig. 8.

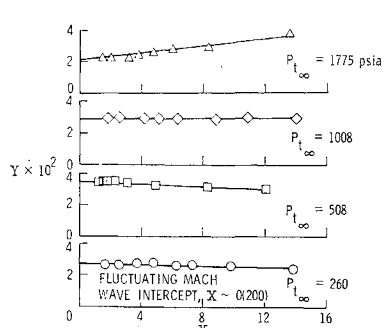

Fig. 9 Fluctuation mode diagrams of freestream disturbances at station 139.

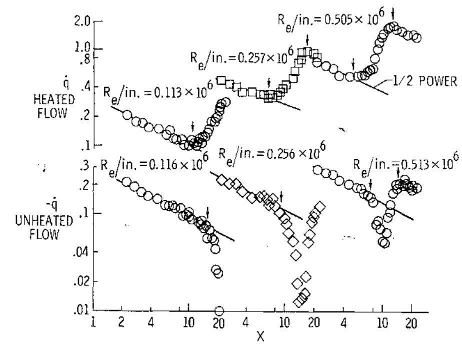

Fig. 10 Method of determining model transition location in heated and unheated flow.

IV. Transition Measurements

The location of the beginning and end of transition was determined from the model heating rate data. The beginning of transition $(R_{e,x})_T$ was defined as the point where $\dot{q}$ departed from a laminar $\frac{1}{2}$-power slope, whereas the beginning of turbulent flow (end of transition) $(R_{e,x})_T$, was taken as the peak heating point (equilibrium turbulent flow occurs downstream of this point). This technique is illustrated in Fig. 10 for both heated ($T_{t_\infty} \approx 790°$R) and unheated flow ($T_{t_\infty} \approx 540°$R). In heated flow the data appear conventional, whereas in unheated flow (when the model cools because the recovery temperature is below room temperature) a sharp drop in $\dot{q}$ marks the beginning of transition. The peculiar drop in $\dot{q}$ for unheated flow probably occurs because of the effect of transition on recovery factor; a realistic assumption for the recovery factor distribution[3] in the transitional flow region was found to give Stanton number vs Reynolds number curves similar to the heated flow curves. The dropoff shown in $\dot{q}$ made it quite easy to accurately determine the transition point. Surface Pitot pressure measurements, obtained by traversing a Pitot tube along the model surface, were also made as a check on the heating rate detection method, and the two techniques gave consistent results.

V. Summary

Laufer[4] has shown that the turbulent nozzle wall boundary layer radiates sound into the tunnel stream, and in a previous section it has been demonstrated that the measured disturbances of the present study (in unheated flow) can be interpreted as sound radiation from the turbulent tunnel wall boundary layer. Both the sound intensity in the tunnel freestream and the transition model results (Reynolds number referenced to local model flow conditions) are therefore summarized in Fig. 11 (also see Table 2 for tabulated results of the transition measurements and a summary of local vs freestream conditions). These results clearly show a strong coupling between the freestream sound intensity and model transition. The inverse correspondence of the two is nearly complete. That is, as the unit Reynolds number is decreased from R_e/in. $\approx 0.6 \times 10^6$ to R_e/in. $\approx 0.2 \times 10^6$, the sound intensity increases and $(R_{e,x})_T$ decreases. From R_e/in. $\approx 0.2 \times 10^6$ to R_e/in. $\approx 0.13 \times 10^6$, both the sound intensity and the $(R_{e,x})_T$ are near constant. In this range of R_e/in., or equivalently P_{t_∞} about 400 psig, transition of the tunnel wall boundary layer is moving through the acoustic origin. Un-

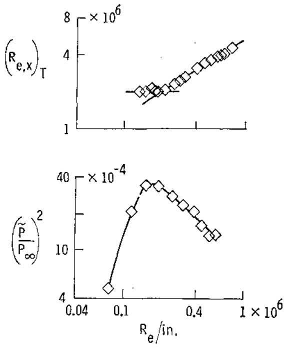

Fig. 11 Effect of freestream disturbances on model transition.

fortunately, $(R_{e,x})_T$ could not be determined at unit Reynolds numbers lower than R_e/in. $\approx 0.13 \times 10^6$ as the presence of the model caused the nozzle boundary layer to separate and impinge on the model at the low stagnation pressures. It was expected that $(R_{e,x})_T$ would increase again below R_e/in. $\approx 0.13 \times 10^6$, since the noise intensity is greatly diminished when the tunnel wall boundary layer approaches laminar. In fact, at R_e/in. $= 0.047 \times 10^6$ ($P_{t_\infty} = 65$ psia) no signal above the instrument noise level could be distinguished.

As the helium tunnel has the unique capability of operating at $M_\infty \approx 20$ in both heated and unheated flow, an attempt was made to repeat the experiments discussed thus far with heated flow ($T_{t_\infty} \approx 790°$R). Unfortunately, the attempts to repeat the hot-wire measurements in heated flow were unsuccessful because of repeated wire failures. It is expected that the use of heated flow could result in temperature spottiness by inadequate mixing in the supply section and could also affect the sound level by changing the characteristics of the tunnel wall boundary layer. Morkovin[16] has pointed out that temperature spottiness may be the "major offender" in heated wind tunnels, and Kovasznay,[1] in fact, concluded that temperature spottiness was the dominant mode in some of his preliminary tests. Therefore, it is suggested that temperature fluctuations should not be arbitrarily ignored in high-temperature wind tunnels when the effects of freestream disturbances on transition are to be determined.

VI. Conclusions

Quantitative hot-wire and boundary-layer transition measurements have been made to determine the nature of the disturbances existing in a hypersonic wind tunnel and the relation of these disturbances to hypersonic boundary-layer transition. For the test conditions of the helium tunnel it was found that:

1) The disturbance fluctuation levels in an unheated hypersonic wind tunnel were quite high, reaching a maximum of 3.5% rms mass flow fluctuation (which corresponds to 6% rms static pressure fluctuation); but only a 0.2% rms total temperature fluctuation, at most, was measured.

2) In unheated flow, the freestream disturbances can be interpreted as sound waves radiating from the turbulent boundary layer on the nozzle wall. For this case the nondimensional sound level increased with decreasing unit Reynolds number. The disturbances were lowest with a laminar boundary layer on the nozzle wall and highest when the boundary layer was transitional.

3) The movement of the model transition point was strongly coupled to the strength of the sound pressure field; the sound intensity was varied by lowering the unit Reynolds number which caused the tunnel wall boundary layer to approach a laminar state. $(R_{e,x})_T$ decreased as the nondimensional sound intensity increased and $(R_{e,x})_T$ was constant when the sound intensity was constant.

Table 2 Summary of transition results on wedge ($T_w \approx 540°$R) unheated flow

P_{t_∞}	M_∞	M_e	R_e/in. $\times 10^6$	T_{t_∞}	$(R_{e,x})_T$	$(R_{e,x})_{T'}$ $\times 10^6$
315	18.1	6.7	0.132	546	1.98	
365	18.3	6.7	0.149	549	2.01	
415	18.5	6.7	0.164	550	2.13	
465	18.7	6.7	0.180	550	1.98	
515	18.9	6.7	0.191	552	2.01	
615	19.3	6.8	0.218	555	2.07	
765	19.6	6.8	0.256	562	2.30	
890	19.9	6.8	0.285	563	2.42	5.58
1015	20.1	6.8	0.316	563	2.62	6.16
1265	20.3	6.8	0.394	567	3.11	7.10
1515	20.5	6.8	0.457	566	3.43	6.85
1765	20.8	6.8	0.513	565	3.64	7.54
2015	21.0	6.8	0.579	566	3.89	7.82
2265	21.2	6.9	0.625	570	4.00	8.44
2515	21.4	6.9	0.671	564	4.09	9.20
3015	21.7	6.9	0.768	582	4.61	10.37

References

[1] Kovasznay, L. S. G., "Turbulence in Supersonic Flow," *Journal of the Aeronautical Sciences*, Vol. 20, No. 10, Oct. 1953, pp. 657–674.

[2] Ribner, H. S. and Tucker, M., "Spectrum of Turbulence in a Contracting Stream," Rept. 1113, 1953, NACA.

[3] Laufer, J., "Factors Affecting Transition Reynolds Numbers on Models in Supersonic Wind Tunnels," *Journal of the Aeronautical Sciences*, Vol. 21, No. 7, July 1954, pp. 497–498.

[4] Laufer, J., "Aerodynamic Noise in Supersonic Wind Tunnels," *Journal of the Aeronautical Sciences*, Vol. 28, No. 9, Sept. 1961, pp. 685–692.

[5] Pate, S. R. and Schueler, C. J., "Effects of Radiated Aerodynamic Noise on Model Boundary-Layer Transition in Supersonic and Hypersonic Wind Tunnels," TR-67-236, 1968, Arnold Engineering Development Center.

[6] Arrington, J. P., Joiner, R. C., Jr., and Henderson, A., Jr., "Longitudinal Characteristics of Several Configurations at Hypersonic Mach Numbers in Conical and Contoured Nozzles," TN D-2498, 1964, NASA.

[7] Morkovin, M. V., "Fluctuations and Hot-Wire Anemometry in Compressible Flows," AGARDograph 24, Nov. 1956.

[8] Dewey, C. F., Jr., "Hot-Wire Measurements in Low Reynolds Number Hypersonic Flows," Memo 63, Sept. 1961, Graduate Aeronautical Lab., California Institute of Technology.

[9] Vrebalovich, T., "Application of Hot-Wire Techniques in Unsteady Compressible Flows," TR-32-229, May 1962, Jet Propulsion Lab., Pasadena, Calif.

[10] Demetriades, A., "Turbulence Measurements in an Axisymmetric Compressible Wake," Publication UG-4118, AF 04(694)-994, Aug. 1967, Philco-Ford Corp., Newport Beach, Calif.

[11] Morkovin, M. V. and Phinney, R. E., "Extended Applications of Hot-Wire Anemometry to High-Speed Turbulent Boundary Layers," AFOSR TN-58-469, ASTIA AD 158-279, June 1958, Johns Hopkins Univ., Dept. of Aeronautics.

[12] Kovasznay, L. S. G., "The Hot-Wire Anemometer in Supersonic Flow," *Journal of the Aeronautical Sciences*, Vol. 17, No. 9, Sept. 1950, pp. 565–572.

[13] Wallace, J. E., "Hypersonic Turbulent Boundary-Layer Studies at Cold Wall Conditions," *Proceedings of the 1967 Heat Transfer and Fluid Mechanics Institute*, edited by P. A. Libby et al., Stanford University Press, 1967, pp. 427–451.

[14] Cohen, N. B., "Boundary-Layer Similar Solutions and Correlation Equations for Laminar Heat-Transfer Distribution in Equilibrium Air at Velocities Up to 41,000 Feet per Second," TR R-118, 1961, NASA.

[15] Laufer, J., Ffowcs Williams, J. E., and Childress, S., "Mechanism of Noise Generation in the Turbulent Boundary Layer," AGARDograph 90, Nov. 1954.

[16] Vrebalovich, T., "Discussion: On Supersonic Wind Tunnels with Low Freestream Disturbances by M. V. Morkovin," *Journal of Applied Mechanics*, Vol. 27, No. 2, June 1960, pp. 362–364.